Supporting Information:

Study of antimicrobial effects of laser-engineered SERS-active Cu@Cu_2O nanostructures and their compatibility with human embryonic kidney cells

Jyotsna Patra,[a] Govind Chouhan,[b] Pratyush Dash,[a] Manika Dandapat,[a] Satyaranjan Satyajit,[a] Umakanta Tripathy,[a] Sheeja Jagadevan,[b] and Amitava Adak*[a]

[a] *Department of Physics, Indian Institute of Technology (Indian School of Mines) Dhanbad-826004, Jharkhand, India. Email: amitavaadak@iitism.ac.in (A. Adak)*
[b] *Department of Environmental Science and Engineering, Indian Institute of Technology (Indian School of Mines) Dhanbad-826004, Jharkhand, India.*

1 Reported works on antibacterial activity using Cu or Cu-based nanoparticles

Table S1 A summary of antibacterial activity using Cu or Cu-based nanoparticles (NPs)

references	Nano-particle	fabrication method, particle size & structure	bacterial strain	Normal cell line	remarks
Shiravand et al.,[1]	Cu NPs	Green synthesis route. Avg. particle size: 22.3 nm	*E.coli*, *S aureus*, etc.	normal human peripheral blood cells	Showed good viability but antibacterial activity at low concentrations ($<$ 100 ug/mL) is absent.
Chen et al.,[2]	Cu@Ag	Chemical reaction method, spherical core-shell nanoparticles	*E.coli* and *S. aureus*	NA	Shown antibacterial activity but cytotoxicity against normal cells is absent.
Dobrucka et al.,[3]	Cu@Pt	Biogenically synthesized by agrimoniae herba extract, particle size 30 nm	Various bacterial strain	NA	Showed various degrees of activity against bacterial strain. cytoxicity against normal cells is absent
Sun et al.,[4]	Carbon nanosheet decorated with Cu@Cu_2O	Hydrothermal method, Cu@Cu_2O particle size in the range 10.5-13.5 nm on 5 nm thick carbon nanosheet	*E.coli* and *S. aureus*	NA	Showed excellent antibacterial activity but at large concentrations(125-1000 ug/mL). Also, biocompatibility is not evaluated.
Our work	Cu@Cu_2O	Pulsed laser ablation (PLA) in deionized water, core-shell nanoparticle of size: $\sim$ 5.6 nm	*E.coli* and *B. pumilus*	Human embryonic kidney (HEK-293)	Shows excellent antibacterial activity against both the bacterial strains at a nanoparticle concentration as low as 5 ug/mL and highly biocompatible upto 25 ug/mL.

2 Quantitative measurements of antibacterial performance of Cu@Cu_2O NPs

Table S2 % Inhibition and log reduction calculated at different concentration of Cu@Cu_2O against *E.coli* and *B.pumilus*. All the experiments were performed in triplicate.

NPs Concentration	% Inhibition		Log reduction	
	Escherichia coli	*Bacillus pumilus*	*Escherichia coli*	*Bacillus pumilus*
C1: 100 μg/mL	99.97 $\pm$ 0.01	99.98 $\pm$ 0.03	3.52 $\pm$ 0.17	3.31*
C2: 75 μg/mL	98.18 $\pm$ 0.38	99.68 $\pm$ 0.09	1.75 $\pm$ 0.09	2.51 $\pm$ 0.13
C3: 50 μg/mL	95.14 $\pm$ 0.77	99.47 $\pm$ 0.17	1.32 $\pm$ 0.07	2.29 $\pm$ 0.14
C4: 25 μg/mL	91.50 $\pm$ 1.57	96.77 $\pm$ 0.42	1.08 $\pm$ 0.08	1.49 $\pm$ 0.06
C5: 5 μg/mL	87.61 $\pm$ 4.20	90.00 $\pm$ 0.57	0.92 $\pm$ 0.14	1.00 $\pm$ 0.03

*In case of *Bacillus pumilus*, with NPs concentration 100 μg/mL, non-zero colony count was found only once were the log reduction could be defined. Hence, error could not be estimated for this case.

3 cell viability (at 24 hr) due to the influence of $Cu@Cu_2O$ NPs performed on HEK-293 cell lines

Table S3 Quantitative details of cell viability and % inhibition at 24 hour

NPs Conc.	Abs.(mean)	Abs. (STD)	% Cell Viability (mean)	% Cell Viability (STD)	% inhibition
5	1.1	0.2	90	15	9
25	1.02	0.05	84	4	15
50	0.6	0.1	52	11	47
75	0.24	0.06	19	4	80
150	0.026	0.004	2.2	0.4	97

* All the experiments were performed in triplicates

4 FFT analysis from TEM images

The FFT analysis is performed on the fringe patterns found in HRTEM images using imageJ software. For this, an HRTEM image (as shown in Figure S1 (a, e and i)) with clear fringe pattern (see Figure S1 (b,f and j))is chosen. FFT image is generated for a selected area of the image with clear fringe pattern. From the FFT (see Figure S1 (c, g and k)), a distinct frequency component (corresponding to the fringe), as indicated by yellow arrow, is chosen to generate a clear IFFT image. The d-spacing is measured from this high contrast IFFT image by taking line-out across the fringe pattern.

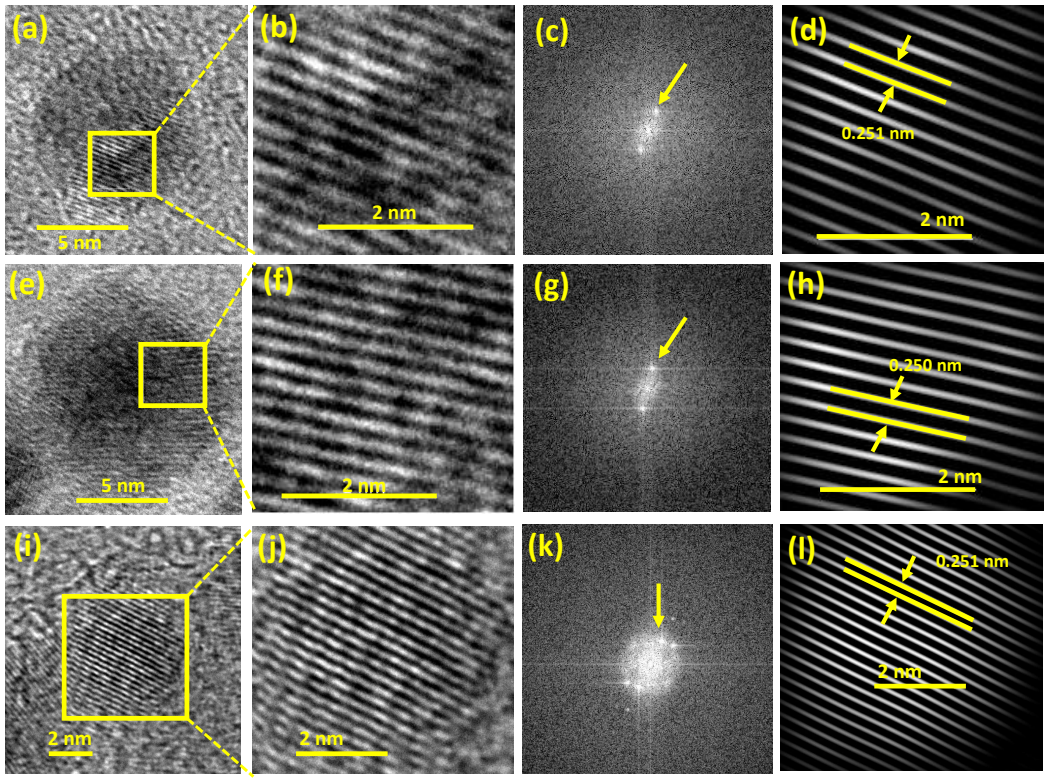

Fig. S1 (a), (e) and (i) HRTEM images of nanoparticle. (b), (f) and (j) enlarged images with visible fringe pattern. (c), (g) and (k) FFTs of the HRTEM images. The distinct frequency component (corresponding to the fringe), as indicated by the yellow arrow, is chosen for each image to generate a clear IFFT image, as shown in (d), (h), and (l), respectively.

5 The d-spacings calculated from obtained SAED pattern

Table S4 d-spacings calculated from obtained SAED pattern

ring no.	d (nm)	hkl
ring 1	0.243	111(Cu_2O)
ring 2	0.207	111(Cu)
ring 3	0.182	002(Cu)
ring 4	0.154	022(Cu_2O)
ring 5	0.131	013(Cu_2O)
ring 6	0.113	123(Cu_2O)

6 Structure of congo red dye molecule

The structure of the Congo red dye molecule is represented in figure below (reference taken from Sigma Aldrich,CAS Number: 573-58-0).

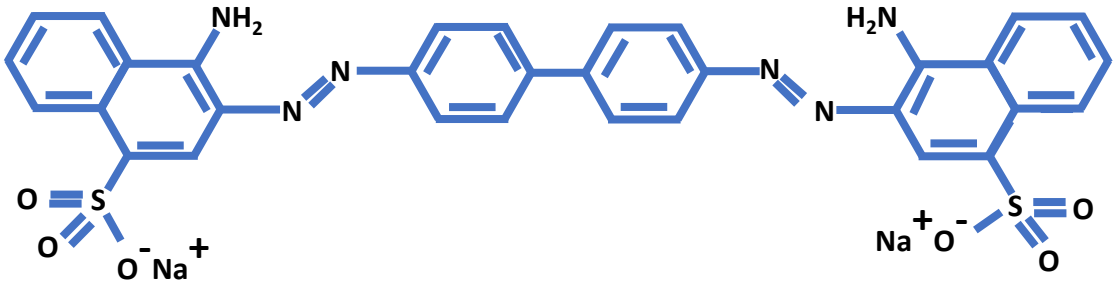

Fig. S2 congo red molecule structure.

7 Assignment of Raman peaks for Congo red dye[5]

Table S5 Raman peak assignment for congo red dye

Raman peak position	Assignment
peak 1: 1593 cm^{-1}	phenyl ring
peak 2: 1452 cm^{-1}	-N=N- stretching
peak 3: 1351 cm^{-1}	Naphthyl ring
peak 4: 1152 cm^{-1}	phenyl-N_{AZO} stretching

8 Previously reported work on SERS analysis of different analyte molecules using Cu or Au/Ag/Cu@Cu_2O nanoparticles

Table S6 A short summary of previously reported work on SERS analysis of different analyte molecules using Cu or Au/Ag/Cu@Cu_2O nanoparticle

ref.	Nanoparticle	particle size & structure	analyte molecule	laser source/ analyte concentration, EF
rawat et al.[6]	Cu in ethylene glycol	3.2-4.3 nm	Methylene blue	514 and 785 nm
Baruah et al.[7]	Cu	12-13 nm	karanjin seed	-
Muniz-miranda et al.[8]	Cu	-	phen and bipy	514 and 785 nm
Wang et al.[9]	Cu, Cu_2O, Cu@Cu_2O	nanodendrites	4- aminobenzenethiol	532 and 633 nm
Chen et al.[10]	Ag@Cu_2O	31 nm shell thickness	4-MBA (mercaptobenzoic acid)	10^{-3} M to 10^{-7} M
Chen et al.[11]	Au@Cu_2O	20 nm core & 48-108 nm shell thickness	MBA (mercaptobenzoic acid)	633 nm(laser power: 1 mW) , 10^{-3} M
Aghdam et al.[12]	Cu@Cu_2O	40 nm	methylene blue and crystal violet	532 nm, 10^{-3} M to 10^{-7} M, EF=1.1 $\times$ 10^5 and 7.5$\times 10^5$ for the CV and MB molecules

9 A comparison of XPS Cu 2p Analysis from Cu, Cu2O and Cu@Cu_2O NPs prepared by different methods in literature with our results

Table S7 A short summary of previously reported work on XPS Cu 2p Analysis from Cu, Cu2O and Cu@Cu_2O

ref.	Cu 2p3/2 peak position (eV)	Cu 2p1/2 peak position (eV)	O 1s peak position (eV)	compound
Tahir et al.[13]	932.5 (Cu_2O) and 932.6 (Cu)	–	530.8	Cu_2O and cu
Yang et al.[14]	932.3	952.5	530	Cu@Cu_2O
Younan et al.[15]	932.5 (Cu_2O) and 932.6/932.7 (Cu)	–	–	Cu_2O and cu
Mao et al.[16]	932.3	952.2	–	Cu_2O/Cu
Ai et al.[17]	932.6	953.1	–	Cu@Cu_2O
Our work	932.5	952.5	531.2	Cu@Cu2O

References

1 S. Shiravand and F. Azarbani, *Green Chemistry Letters and Reviews*, 2017, **10**, 241–249.
2 K.-t. Chen, D. Ray, Y.-h. Peng and Y.-C. Hsu, *Current Applied Physics*, 2013, **13**, 1496–1501.
3 R. Dobrucka and J. Dlugaszewska, *Saudi pharmaceutical journal*, 2018, **26**, 643–650.
4 G. Sun, S. Jia, X. Zhang, Z. Kang, M. Cui, B. Wang, B. Wang and D.-P. Yang, *ACS Applied Nano Materials*, 2021, **4**, 9831–9841.
5 C. E. Bonancêa, G. M. do Nascimento, M. L. De Souza, M. L. Temperini and P. Corio, *Applied Catalysis B: Environmental*, 2006, **69**, 34–42.
6 R. Rawat, A. Tiwari, M. K. Singh, R. Mandal, A. Pathak and A. Tripathi, *Radiation Effects and Defects in Solids*, 2020, **175**, 332–341.
7 P. K Baruah, A. Singh, I. Jahan, L. Rangan, A. N Panda, A. K Sharma and A. Khare, *Advanced Materials Letters*, 2017, **8**, 971–976.
8 M. Muniz-Miranda, C. Gellini and E. Giorgetti, *The Journal of Physical Chemistry C*, 2011, **115**, 5021–5027.
9 R.-C. Wang and C.-H. Li, *Acta materialia*, 2011, **59**, 822–829.

10 L. Chen, H. Sun, Y. Zhao, Y. Zhang, Y. Wang, Y. Liu, X. Zhang, Y. Jiang, Z. Hua and J. Yang, *RSC advances*, 2017, **7**, 16553–16560.
11 L. Chen, F. Zhang, X.-Y. Deng, X. Xue, L. Wang, Y. Sun, J.-D. Feng, Y. Zhang, Y. Wang and Y. M. Jung, *Spectrochimica Acta Part A: Molecular and Biomolecular Spectroscopy*, 2018, **189**, 608–612.
12 H. D. Aghdam, S. M. Bellah and R. Malekfar, *Spectrochimica Acta Part A: Molecular and Biomolecular Spectroscopy*, 2019, **223**, 117379.
13 D. Tahir and S. Tougaard, *Journal of physics: Condensed matter*, 2012, **24**, 175002.
14 X. Yang, J. Cheng, X. Yang, Y. Xu, W. Sun and J. Zhou, *Chemical Engineering Journal*, 2022, **431**, 134171.
15 H. Younan, S. Yue, L. Kai, W. J. Yuan, C. Y. Shen, C. Yixin, F. Chao and L. Xiaomin, 2016 IEEE 37th International Electronics Manufacturing Technology (IEMT) & 18th Electronics Materials and Packaging (EMAP) Conference, 2016, pp. 1–2.
16 P. Mao, L. Qi, X. Liu, Y. Liu, Y. Jiao, S. Chen and Y. Yang, *Journal of hazardous materials*, 2017, **328**, 21–28.
17 Z. Ai, L. Zhang, S. Lee and W. Ho, *The Journal of Physical Chemistry C*, 2009, **113**, 20896–20902.